Measurement of the valence band offset in novel heterojunction systems: Si/Ge (100) and AlSb/ZnTe (100)

E. T. Yu, E. T. Croke, D. H. Chow, D. A. Collins, M. C. Phillips, T. C. McGill, and J. O. McCaldin
T. J. Watson, Sr., Laboratory of Applied Physics, California Institute of Technology, Pasadena, California 91125

R. H. Miles
Hughes Research Laboratories, Malibu, California 90265

(Received 30 January 1990; accepted 14 March 1990)

We have used x-ray photoelectron spectroscopy to measure the valence band offset *in situ* for strained Si/Ge (100) heterojunctions and for AlSb/ZnTe (100) heterojunctions grown by molecular-beam epitaxy. For the Si/Ge system, Si 2*p* and Ge 3*d* core level to valence band edge binding energies and Si 2*p* to Ge 3*d* core level energy separations were measured as functions of strain, and strain configurations in all samples were determined using x-ray diffraction. Our measurements yield valence band offset values of 0.83 ± 0.11 eV and 0.22 ± 0.13 eV for Ge on Si (100) and Si on Ge (100), respectively. If we assume that the offset between the weighted averages of the light-hole, heavy-hole, and spin-orbit valence bands in Si and Ge is independent of strain, we obtain a discontinuity in the average valence band edge of 0.49 ± 0.13 eV. For the AlSb/ZnTe (100) heterojunction system, we obtain a value of -0.42 ± 0.07 eV for the valence band offset. Our data also suggest that an intermediate compound, containing Al and Te, is formed at the AlSb/ZnTe (100) interface.

I. INTRODUCTION

The use of x-ray photoelectron spectroscopy (XPS) to measure the valence band offset in lattice-matched heterojunctions has been well-established.[1,2] However, many materials systems of current interest are characterized by a substantial lattice mismatch, leading to a dependence of the valence band offset on the strain configuration in the heterojunction. In addition, it has been pointed out by Tersoff and Van de Walle[3] and by Schwartz *et al.*[4] that core level to valence band edge binding energies are, in principle, functions of strain, and that this dependence must be included in any measurement of band offsets in strained heterojunctions using XPS.

In this paper, we present the results of measurements of the valence band offset in strained Si/Ge (100) heterojunctions using XPS. The Si/Ge heterojunction system was particularly appropriate for this type of study, because of the large lattice mismatch (4.18%) between Si and Ge, and because the conditions under which coherently strained epilayers can be grown are well-known.[5,6] In addition, theoretical calculations of the Si/Ge band offset have been performed that explicitly incorporate the effects of strain;[7] these calculations, as well as earlier experimental work,[4,8] indicate that strain strongly influences the value of the valence band offset. Si/Ge interfaces are also of interest from a technological point of view, because of the possibility of integrating devices utilizing Si/Ge heterojunctions directly into existing Si-based structures. Band offset values are critical in determining the properties, and often even the feasibility, of tunnel structures,[9] superlattice-based devices,[10] and other electronic and optoelectronic devices.

We also present the results of XPS measurements of the valence band offset for the AlSb/ZnTe (100) heterojunction system. The AlSb/ZnTe heterojunction is of particular relevance for a recently proposed visible light emitting structure utilizing *n*-AlSb/*p*-ZnTe heterojunctions.[11] The value of the AlSb/ZnTe band offset is a critical parameter in determining the feasibility of these devices.

II. Si/Ge (100) VALENCE BAND OFFSET

Figures 1(a) and 1(b) show schematic energy-band diagrams for Ge coherently strained to Si (100) and Si coherently strained to Ge (100), respectively. As shown in these figures, the valence band offset is given by

$$\Delta E_v = (E^{\mathrm{Ge}}_{\mathrm{Ge}\,3d} - E^{\mathrm{Ge}}_{v}) + (E^{\mathrm{Si}}_{\mathrm{Si}\,2p} - E^{\mathrm{Ge}}_{\mathrm{Ge}\,3d}) - (E^{\mathrm{Si}}_{\mathrm{Si}\,2p} - E^{\mathrm{Si}}_{v}). \quad (1)$$

The biaxial strain in the Ge layer in Fig. 1(a) and in the Si layer in Fig. 1(b) produces a splitting of the light-hole, heavy-hole, and spin-orbit valence bands, and a strain-dependent shift in the atomic core level to valence band edge binding energies. This dependence of core level binding energies on strain must therefore be included, either experimentally or theoretically, in measurements of both the bulk core level binding energies and the heterojunction core level energy separations if one hopes to obtain meaningful results for the valence band offset.

The samples prepared for this study were grown by molecular-beam epitaxy (MBE) in a Perkin-Elmer 430S Si MBE system. The base pressure of the growth chamber was typically $\sim 8 \times 10^{-11}$ Torr, and growth pressures were typically near 2×10^{-9} Torr. Samples were grown on *n*-type (100) Si substrates (P-doped to 0.02 to 0.60 Ω cm). The substrate cleaning and oxide desorption procedures are described elsewhere.[12] Following oxide desorption, a 1200 Å Si buffer layer was grown on each substrate as the substrate temperature

 0734-211X/90/040908-08$01.00

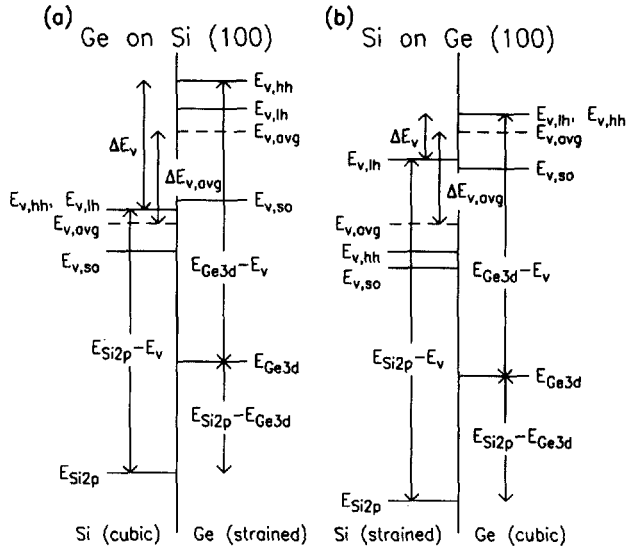

FIG. 1. Schematic energy band diagrams for (a) Ge coherently strained to Si (100) ($a_{\parallel} = 5.431$ Å), and (b) Si coherently strained to Ge (100) ($a_{\parallel} = 5.658$ Å). Valence band splittings result from strain and spin-orbit interactions. Weighted averages of the valence bands in each material are indicated by the dashed lines.

dropped from 700 to 530 °C to ensure an atomically smooth (100) Si starting surface.

Three types of samples were grown for this experiment. To measure the Si 2*p* core level to valence band edge binding energy as a function of strain, four samples were grown, each consisting of a 5000 Å layer of Ge grown at 500 °C, followed by a 5000 Å layer of $Si_{1-x}Ge_x$ with x varying from 0.00 to 0.30, also grown at 500 °C; the samples were annealed at 700 °C for 30 min after each of these layers was grown. The alloy layer was followed by a thin (300 to 1000 Å) layer of Si grown at 310 °C. The Ge and $Si_{1-x}Ge_x$ layers were intended to be fully relaxed to their natural lattice constants; the Ge layers were present to help ensure that the $Si_{1-x}Ge_x$ alloy layers were indeed fully relaxed. The top Si layer was intended to be coherently strained to the in-plane lattice constant of the alloy layer; the Si layer thicknesses were therefore kept well below the critical thickness for strain relaxation,[5] and a lower growth temperature was used.[6]

To measure the Ge 3*d* core level to valence band edge binding energy as a function of strain, a similar series of five samples was grown. Each sample consisted of a 5000 Å layer of $Si_{1-x}Ge_x$ with x varying from 0.70 to 1.00, grown at 500 °C and annealed at 700 °C for 30 min, followed by a thin (300 to 1000 Å) layer of Ge grown at 310 °C. The $Si_{1-x}Ge_x$ layers were intended to be fully relaxed to their natural lattice constants; the intervening Ge layer was not required for these samples, since the alloys were sufficiently Ge-rich to ensure that the critical thicknesses for strain relaxation were much less than the 5000 Å film thickness. The top Ge layer was intended to be coherently strained to the in-plane lattice constant of the alloy layer.

The strain dependence of the Si 2*p* to Ge 3*d* core level energy separation was obtained from measurements on pure Si/Ge (100) superlattices of varying composition coherently strained to relaxed $Si_{1-x}Ge_x$ alloy layers with the same average composition as the superlattice. Each sample consisted of a 2000 Å Si/Ge superlattice grown at 310 °C, on top of a 5000 Å $Si_{1-x}Ge_x$ alloy layer, grown at 500 °C. The Si-rich alloys ($x < 0.50$) were grown on top of a 5000 Å layer of Ge, grown at 500 °C, to help ensure that the alloy layers were fully relaxed; the Ge-rich alloy layers were grown directly on the Si buffer layer.

XPS measurements were obtained using a Perkin-Elmer model 5100 analysis system with a monochromatic Al $K\alpha$ x-ray source ($h\nu = 1486.6$ eV). The analysis chamber is connected to the Si MBE growth chamber via an ultrahigh vacuum (UHV) transfer tube, allowing samples to be grown and analyzed without being exposed to atmosphere. Representative XPS spectra from bulk Si, bulk Ge, and Si/Ge superlattice samples are shown in Figs. 2(a)–2(c), respectively. The discontinuities in the spectra at 4 eV in Figs. 2(a) and 2(b) are due to the longer sampling time near the valence band edge; the valence band spectra for these samples are also shown on enlarged scales, as indicated in the figures.

Core level peak positions were obtained by subtracting from each core level peak a background function proportional to the integrated photoelectron intensity, and defining the peak position to be the midpoint of the two energies at which the intensity was one-half the maximum intensity. The uncertainty in measured core level energy separations was estimated to be ± 0.02 eV, and measurements of core

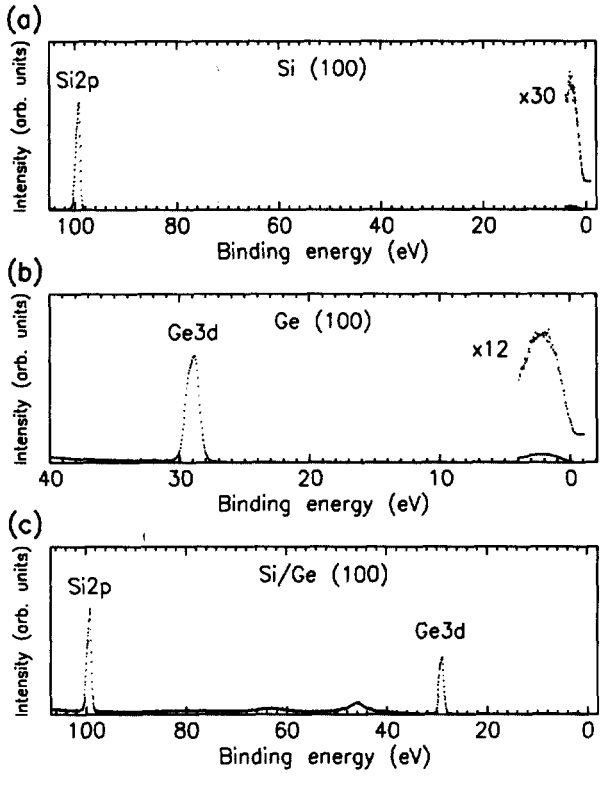

FIG. 2. Representative binding energy XPS spectra for (a) Si (100) samples, (b) Ge (100) samples, and (c) Si/Ge (100) superlattices. The discontinuities in the spectra in (a) and (b) are due to longer sampling times used in the vicinity of the valence bands. The valence band spectra are also shown on enlarged intensity scales, as indicated in the figures.

level energy separations were typically reproducible to better than $\pm$ 0.01 eV. The position of the valence band edge in each XPS spectrum was determined using the precision analysis technique of Kraut *et al.*,[13] modified to include effects due to strain on the valence band density of states. In this approach, the XPS spectrum near the valence band is modeled as a convolution of a theoretical valence band density of states with an experimentally determined XPS instrumental resolution function. This model function is then fitted to the experimental data to give the position of the valence band edge. The valence band densities of states for Si and Ge were calculated using the empirical pseudopotential method;[14] spin-orbit interactions[15] and a nonlocal electron effective mass parameter[16] were included in these calculations. Strain effects were incorporated in the densities of states by performing a Pikus-Bir transformation on the Hamiltonian,[17] and fitting the resulting splitting of the valence bands to known deformation potentials for Si and Ge.[18] Typical XPS valence band spectra, model curves fitted to the data, and calculated valence band densities of states for unstrained Si and Ge are shown in Figs. 3(a) and 3(b), respectively. The uncertainty in core level to valence band edge binding energies was taken to be $\pm$ 0.04 eV; for a given sample, however, measurements were typically reproducible to better than $\pm$ 0.01 eV.

X-ray rocking curve measurements were performed on the strained Si and Ge samples using a Blake Industries high-resolution spectrometer equipped with a Philips four-crystal monochromator. Rocking curve measurements were obtained for the (422) reflection, allowing both the growth-direction and in-plane lattice constants of the relaxed alloy layers and the strained Si and Ge layers to be determined. The x-ray diffraction spectra indicated that the alloy layers were always nearly fully relaxed, and that, on average, approximately 81% of the lattice mismatch between the pure Si or Ge layers and the underlying alloy was accommodated by strain.

The strain configurations in the superlattice samples were determined from $\theta/2\theta$ x-ray diffraction measurements. The diffraction spectra contained (400)-like superlattice peaks, from which the superlattice period and average composition were deduced. This information, combined with known growth rates for the individual Si and Ge layers in the superlattice, was consistent with the superlattices being coherently strained to the underlying alloy layers.

Si 2*p* core level binding energies, Ge 3*d* core level binding energies, and Si 2*p* to Ge 3*d* core level energy separations as functions of the in-plane lattice constant $a_{\parallel}$ have been plotted in Figs. 4(a)–4(c), respectively. The lines in each figure were obtained from least-squares fits to the plotted data points. The core level binding energies and core level energy separations were found to be

$$E^{\mathrm{Si}}_{\mathrm{Si}\,2p} - E^{\mathrm{Si}}_{v} = 98.95 + 1.96(a_{\parallel} - 5.431), \tag{2a}$$

$$E^{\mathrm{Ge}}_{\mathrm{Ge}\,3d} - E^{\mathrm{Ge}}_{v} = 29.41 - 1.24(a_{\parallel} - 5.658), \tag{2b}$$

$$E^{\mathrm{Si}}_{\mathrm{Si}\,2p} - E^{\mathrm{Ge}}_{\mathrm{Ge}\,3d} = 70.09 + 0.526(a_{\parallel} - 5.431), \tag{2c}$$

where energies are in electron volts and $a_{\parallel}$ is in angstroms.

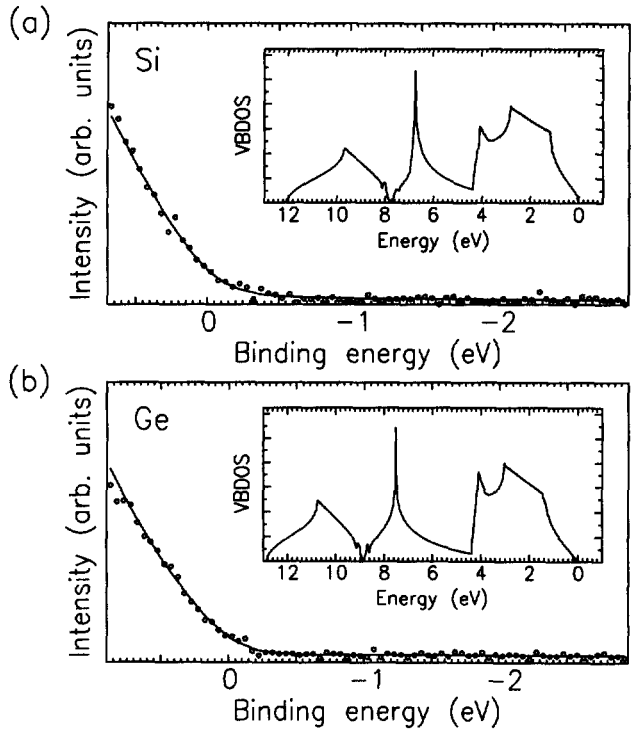

FIG. 3. Typical XPS valence band spectra and model functions fitted to the experimental data for (a) unstrained Si and (b) unstrained Ge. The theoretical valence band densities of states used to construct the model functions are shown in the insets to each figure.

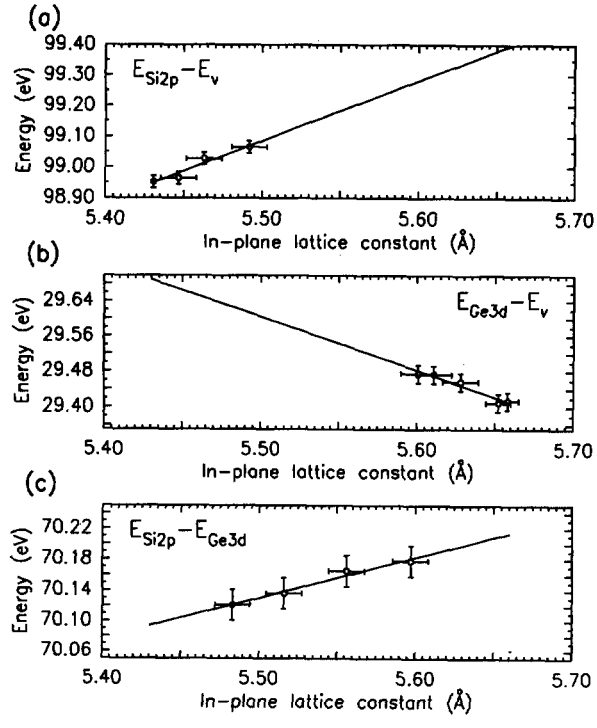

FIG. 4. Core level to valence band edge binding energy differences as a function of the in-plane lattice constant for (a) the Si 2*p* core level in strained Si (100), and (b) the Ge 3*d* core level in strained Ge (100). The Si 2*p* to Ge 3*d* core level energy separation as a function of the in-plane lattice constant in Si/Ge (100) superlattices is shown in (c). The valence band offset in strained Si/Ge (100) heterojunctions is obtained from these three parameters.

For the strained Si and Ge films, $a_{\parallel}$ was determined directly from x-ray diffraction measurements; the superlattices were assumed to be coherently strained to the alloy layers, in accord with the $\theta/2\theta$ diffraction measurements previously described. Combining these results, we obtain valence band offsets of 0.83 ± 0.11 eV and 0.22 ± 0.13 eV for Ge on Si (100) ($a_{\parallel} = 5.431$ Å) and Si on Ge (100) ($a_{\parallel} = 5.658$ Å), respectively. If we assume that the offset between the weighted averages of the light-hole, heavy-hole, and spin-orbit valence bands in Si and Ge is independent of strain,[7] we obtain a discontinuity in the average valence band edge of 0.49 ± 0.13 eV. Uncertainties in the strain-dependent core level binding energies and core level energy separations were determined in the fitting procedure, assuming uncertainties of ± 0.02 eV in binding energy measurements between samples, and an uncertainty of approximately ± 0.01 Å in $a_{\parallel}$ for each sample. An additional uncertainty of ± 0.04 eV was estimated for the core level to valence band edge binding energies, independent of strain. These uncertainties were added in quadrature to obtain the total uncertainty in the valence band offsets.

The values obtained for the valence band offset are in fairly good agreement with the calculations of Van de Walle and Martin,[7] who report values of 0.84 eV for Ge on Si (100), and 0.31 eV for Si on Ge (100). In a recent XPS experiment, Schwartz *et al.*[4] calculated strain shifts in the core level binding energies and measured core level energy separations in strained Ge on Si (100) and Si on Ge (100), obtaining valence band offsets of 0.74 ± 0.13 eV and 0.17 ± 0.13 eV for the two cases, respectively. The strain dependence of their band offsets agrees well with our observations, although the actual band offset values are shifted by ~ 0.1 eV. Several experiments have also been performed to measure band offsets for heterojunctions in which the strain configuration was unknown, and in which a substantial number of dislocations may have been present. Kuech *et al.*[19] obtained $\Delta E_v = 0.39 \pm 0.04$ eV for Ge on Si (100) from reverse-bias capacitance measurements; using photoemission spectroscopy, Margaritondo *et al.*[20] obtained $\Delta E_v = 0.2$ eV for Ge on Si (111), and Mahowald *et al.*[21] obtained $\Delta E_v = 0.4 \pm 0.1$ eV for Si on Ge (111).

Attempts have also been made to observe modulation doping in $Si/Si_{1-x}Ge_x$ heterostructures, and the results of these experiments provide qualitative information on band offsets for these heterojunctions. People *et al.*[22] have observed modulation doping effects for holes in $Si/Si_{0.8}Ge_{0.2}$ heterojunctions coherently strained to Si (100); their experiments suggest that the valence band edge in the alloy is significantly higher in energy than that in the Si layer, allowing holes to be confined in the alloy layer. Using the interpolation scheme of Van de Walle and Martin to obtain band offsets for heterojunctions involving SiGe alloys in intermediate strain configurations, we find that our measurements correspond to $\Delta E_v = 0.16$ eV and $\Delta E_c = -0.02$ eV; these values are consistent with People's results. Abstreiter *et al.*[23] observed enhanced electron mobilities in $Si/Si_{0.5}Ge_{0.5}$ superlattices coherently strained to a $Si_{0.75}Ge_{0.25}$ buffer layer when the $Si_{0.5}Ge_{0.5}$ superlattice layers were doped. For this heterojunction system, our measurements correspond to a valence band offset of 0.28 eV and a conduction band offset of 0.14 eV, consistent with Abstreiter's results.

III. AlSb/ZnTe (100) VALENCE BAND OFFSET

A schematic energy band diagram for the AlSb/ZnTe heterojunction is shown in Fig. 5. Strain-induced effects on the electronic structure of the two materials are neglected due to the small lattice mismatch (0.55%) between AlSb and ZnTe. As shown in the figure, the valence band offset is given by

$$\Delta E_v = (E^{\mathrm{AlSb}}_{\mathrm{Al}\,2p} - E^{\mathrm{AlSb}}_{v}) - (E^{\mathrm{ZnTe}}_{\mathrm{Zn}\,3d} - E^{\mathrm{ZnTe}}_{v}) - (E^{\mathrm{AlSb}}_{\mathrm{Al}\,2p} - E^{\mathrm{ZnTe}}_{\mathrm{Zn}\,3d}). \quad (3)$$

The samples prepared for this study were grown by MBE in two Perkin-Elmer 430P MBE systems; the AlSb layers were grown in a chamber dedicated to the growth of III–V semiconductors, and the ZnTe layers were grown in a chamber devoted to II–VI semiconductor growth. All samples were grown on *p*-type ($p \sim 1 \times 10^{17}$ cm^{-3}) GaSb (100) substrates. Following oxide desorption at 530 °C, a GaSb buffer layer was grown at 100 Å/min, with the substrate at 475 °C. AlSb layers were grown at 62.5 Å/min and with a substrate temperature of 530 °C; for the ZnTe layers, a growth rate of 50 Å/min and a substrate temperature of 270 °C were used.

Al 2*p* core level to valence band edge binding energies were measured in two 5000 Å AlSb layers grown on the GaSb buffers. Both AlSb films displayed very good (1×3) reflection high energy electron diffraction (RHEED) patterns. To measure the Al 2*p* to Zn 3*d* core level energy sepa-

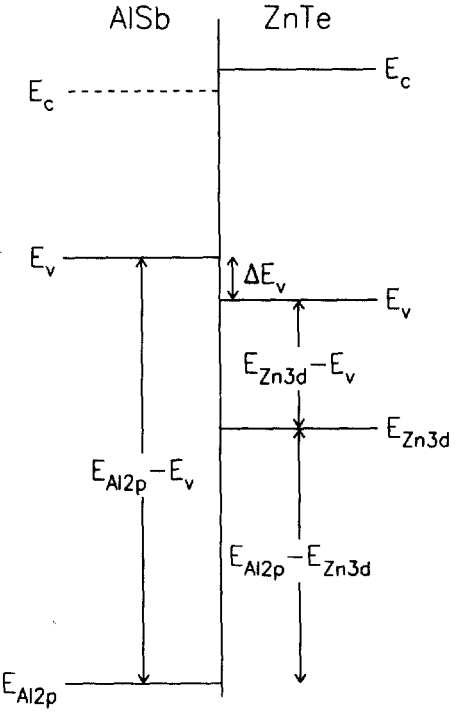

FIG. 5. A schematic energy band diagram for the AlSb/ZnTe heterojunction. The band gap in AlSb is indirect, as indicated by the dashed line representing the AlSb conduction band edge.

ration, two samples were grown. Each consisted of over 5000 Å of AlSb grown on the GaSb buffer layer, followed by ~25 Å of ZnTe. Streaky RHEED patterns were observed 5 to 10 s (~3 to 9 Å) after the ZnTe growths were begun, indicating that growth was two dimensional. For the Zn 3*d* core level binding energy measurement, an additional 250 Å layer of ZnTe was grown on each AlSb/ZnTe heterojunction sample after the XPS core level energy separation measurements had been made. The heterojunction samples showed relatively little sign of surface deterioration following the XPS measurements, and streaky ZnTe RHEED patterns were observed almost immediately after growth of ZnTe commenced. The final ZnTe surfaces all yielded good (2×1) RHEED patterns. Growth of the bulk ZnTe and AlSb/ZnTe heterojunction samples required the use of both growth chambers, with the samples being transported between the two systems under UHV conditions. Immediately following all growths, the samples were transported under UHV conditions to the XPS chamber for analysis.

Sample XPS spectra for bulk AlSb, bulk ZnTe, and AlSb/ZnTe heterojunctions are shown in Figs. 6(a)–6(c), respectively. The valence band spectra for the bulk AlSb and ZnTe samples are also shown on enlarged scales, as indicated in the figure. The Al 2*p* and Zn 3*d* bulk core level positions and the AlSb and ZnTe valence band edge positions were determined using the methods described in Sec. II. The positions of the spin-orbit resolved Sb 4*d* and Te 4*d* peaks were determined by fitting the core level spectra, following background subtraction, to characteristic peak shape functions consisting of two identically shaped Voigt functions separated by a fixed spin-orbit splitting, whose relative heights scaled as $(2J+1)$.

Measurements obtained from the bulk AlSb samples yielded an Al 2*p* core level to valence band edge binding energy of 72.92 ± 0.04 eV. Our measurement is in good agreement with a previously reported value[24] of 72.96 eV. The separation between the Al 2*p* and Sb $4d_{5/2}$ core levels in AlSb was found to be 41.72 ± 0.02 eV; comparison of the Al 2*p* to Sb $4d_{5/2}$ core level energy separation in bulk and heterojunction samples provides one way to confirm that core level binding energies are indeed bulk properties, and are not significantly influenced by the presence of the interface in a heterojunction sample.

For the bulk ZnTe samples, we obtained values of 9.42 ± 0.04 eV and 30.02 ± 0.02 eV for the Zn 3*d* core level to valence band edge binding energy and the Te $4d_{5/2}$ to Zn 3*d* core level energy separation, respectively. Reported values[25] for the Zn 3*d* core level to valence band edge binding energy range from 9.1 to 9.84 eV. Figures 7(a) and 7(b) show the valence band spectra, model functions fitted to the XPS data, and calculated valence band densities of states for AlSb and ZnTe, respectively.

Determination of the Al 2*p* to Zn 3*d* core level energy separation in the AlSb/ZnTe heterojunctions was complicated by the apparent formation of a reacted layer at the AlSb/ZnTe interface. Evidence of this reaction can be seen in the spectra for the Al 2*p*, Sb 4*d*, and Te 4*d* core levels. Figures 8(a) and 8(b) show Sb 4*d* core level spectra for bulk AlSb and an AlSb/ZnTe heterojunction, respectively. The bulk AlSb spectrum contains a small component at higher binding energy compared to the main peak; an analogy with

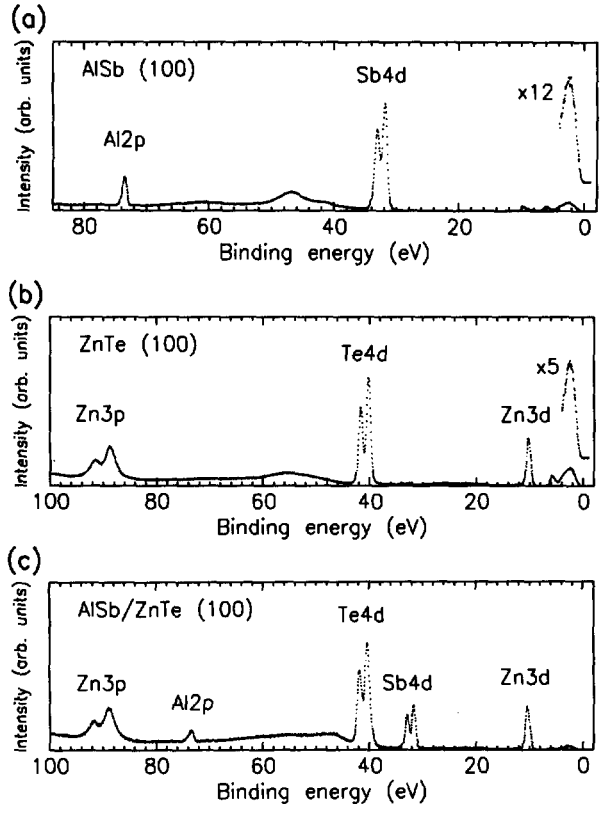

FIG. 6. Representative binding energy XPS spectra for (a) AlSb (100), (b) ZnTe (100), and (c) an AlSb/ZnTe (100) heterojunction. The AlSb and ZnTe valence band spectra in (a) and (b), respectively, are also shown on enlarged intensity scales, as indicated in the figures.

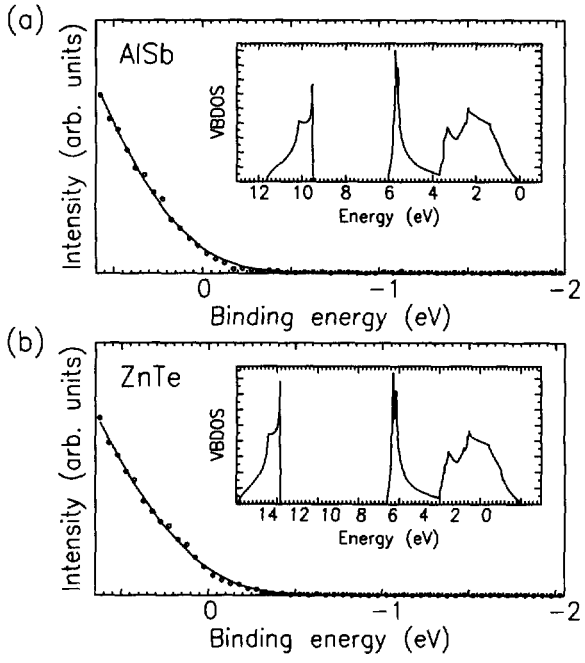

FIG. 7. Typical XPS valence band spectra and model functions fitted to the experimental data for (a) AlSb and (b) ZnTe. The theoretical valence band densities of states used to construct the model functions are shown in the insets to each figure.

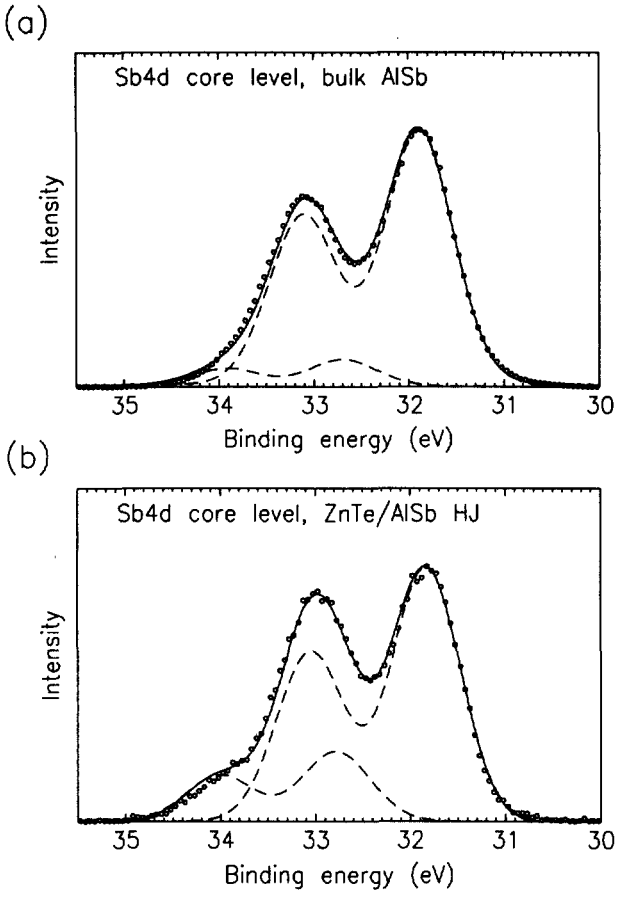

FIG. 8. Sb 4*d* core level XPS spectra from (a) bulk AlSb and (b) a ZnTe/AlSb heterojunction. In (a), the small peak shifted to higher binding energy with respect to the bulk peak is thought to be due to excess Sb on the AlSb surface. In (b), the peak shifted to higher binding energy was found to originate from Sb at the sample surface, i.e., on top of the ZnTe layer.

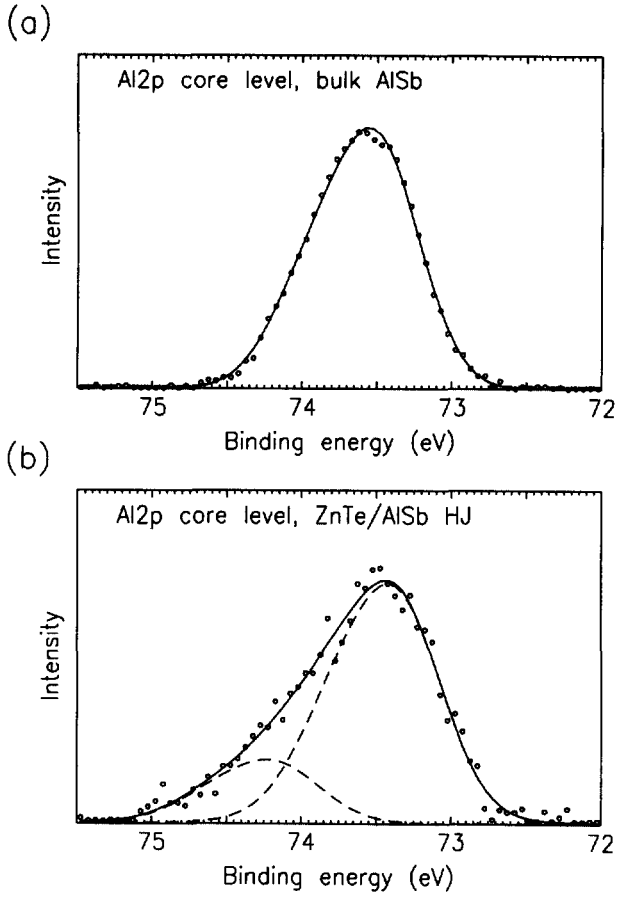

FIG. 9. Al 2*p* core level XPS spectra from (a) bulk AlSb and (b) a ZnTe/AlSb heterojunction. The bulk AlSb peak in (a) does not contain any chemically shifted components. The heterojunction spectrum in (b) clearly contains a component shifted to higher binding energy, indicating that Al bonding to Te is present in the reacted layer at the AlSb/ZnTe interface.

observed surface core level shifts in the As-rich $c(4\times4)$ reconstruction of GaAs[26] suggests that this component may be due to excess Sb on the AlSb surface. The spectrum recorded from the heterojunction sample clearly shows a peak shifted to higher binding energy relative to the main peak structure. By varying the electron take-off angle from the sample, and therefore the effective electron escape depth, we were able to determine that the smaller, shifted peak was due to Sb on the surface of the sample, i.e., on top of the thin ZnTe layer. This conclusion is also supported by the presence of a small but detectable Sb 4*d* core level peak even for samples with 275 Å ZnTe deposited on AlSb.

The Al 2*p* core level spectrum from an AlSb/ZnTe heterojunction, shown in Fig. 9(b), also exhibits a peak shifted to higher binding energy; the shifted peak is not present in the spectrum shown in Fig. 9(a), obtained from bulk AlSb. Electronegativity arguments would suggest that Al in the reacted layer forms bonds with Te, in which case a peak shifted to lower binding energy should appear in the Te 4*d* spectrum from an AlSb/ZnTe heterojunction. Figures 10(a) and 10(b) show Te 4*d* core level spectra from bulk ZnTe and an AlSb/ZnTe heterojunction, respectively, and a peak shifted to lower binding energy does indeed appear in the heterojunction spectrum. The Te 4*d* spectra also contain very small peaks shifted to higher binding energy; as with the bulk AlSb spectra, these peaks may be due to excess Te on the ZnTe surface. The compound most likely to be forming at the interface is Al_2Te_3.

The chemical behavior at the AlSb/ZnTe interface thus appears to be very similar to that observed in GaSb/ZnTe heterojunctions, in which a reacted layer containing Ga and Te is formed at the GaSb/ZnTe interface. A layer of Ga_2Se_3 in the wurtzite phase has also been observed to form at the GaAs/ZnSe (110) interface.[27] The effect of the reacted layer on the electronic structure of the interface is unknown but may be significant, and deserves further study. The presence of the reacted layer may also have implications for the structural properties, such as strain configuration, of the heterojunction.

The presence of a large shifted peak in the Al 2*p* core level spectrum complicates the determination of the Al 2*p* to Zn 3*d* core level energy separation. To ensure that the position assigned to the Al 2*p* core level corresponded to that in bulk AlSb and was not affected by the presence of the chemically shifted component in the spectrum, we checked the energy separation between the Al 2*p* core level peak components and the Sb 4*d* peak components. By requiring this energy separation to be equal in the bulk AlSb and heterojunc-

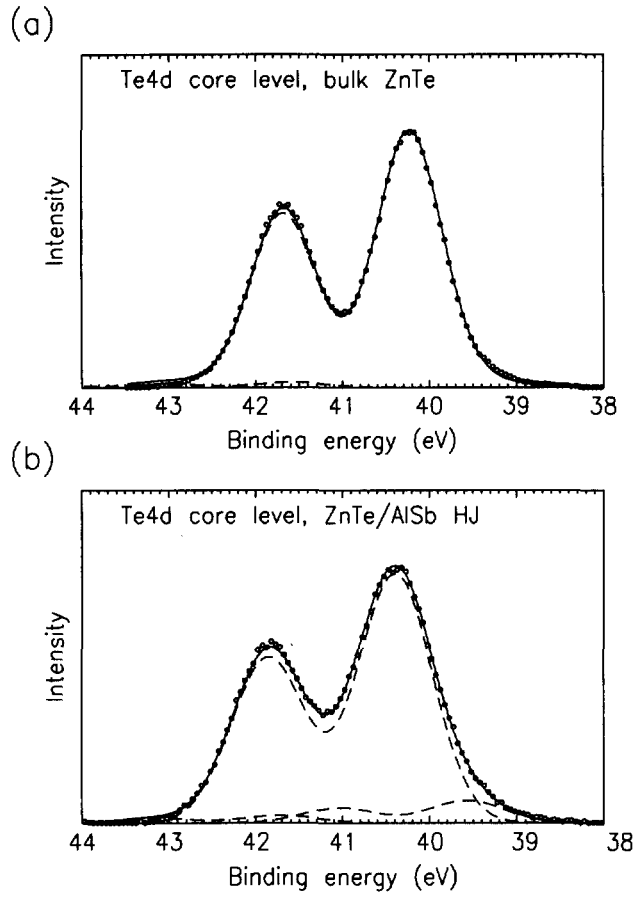

FIG. 10. Te 4*d* core level XPS spectra from (a) bulk ZnTe and (b) a ZnTe/AlSb heterojunction. Both spectra contain a small peak shifted to higher binding energy with respect to the main peak; this peak may originate from excess Te at the surface. The heterojunction spectrum also contains a peak shifted to lower binding energy, indicating that Te bonding to Al is present in the reacted layer at the AlSb/ZnTe interface.

tion samples, we were able to identify unambiguously the peak components corresponding to the pure AlSb layer in the heterojunction. The Zn 3*d* core level spectrum did not appear to contain a significant chemically shifted component; the Zn 3*d* core level position was therefore determined using the simple method of Sec. II, and the Zn 3*d* to Te $4d_{5/2}$ core level energy separation was confirmed to be the same as that in bulk ZnTe.

We obtained a value of 63.08 ± 0.04 eV for the Al 2*p* to Zn 3*d* core level energy separation; the uncertainty in this measurement was due largely to the presence of the chemically shifted component in the Al 2*p* core level spectrum. Combining this with the measurements of the Al 2*p* and Zn 3*d* core level to valence band edge binding energies, we obtain a valence band offset ΔE_v(AlSb/ZnTe) $= -0.42 \pm 0.07$ eV. The corresponding conduction band offset is $\Delta E_c = 0.21 \pm 0.07$ eV. The band alignment is therefore type I, as shown schematically in Fig. 5. Theoretically predicted values for this band offset encompass a wide range of values. Tersoff[28] predicts $\Delta E_v = 0.39$ eV, and the electron affinity rule[29] yields $\Delta E_v = 0.48$ eV. However, Harrison's linear combination of atomic orbitals (LCAO) theory[30] gives $\Delta E_v = 0.83$ eV, and Harrison and Tersoff[31] obtain $\Delta E_v = 1.17$ eV. The serious discrepancies among these theories attest to the need for reliable experimental measurements of band offsets in AlSb/ZnTe and other novel heterojunction systems.

Our measurement also has implications for the viability of *n*-AlSb/*p*-ZnTe light emitting devices. In their original proposal, McCaldin and McGill[11] argue that efficient electron injection from AlSb into ZnTe will be difficult to achieve if the conduction band offset is too large; high doping levels in the AlSb layers are also required, unless the conduction band offset is small, e.g., $\Delta E_c < 0.2$ eV. Recent efforts[32] to dope AlSb using PbTe have resulted in *n*-type AlSb with carrier concentrations up to $\sim 9 \times 10^{17}$ cm^{-3}. A conduction band offset of 0.21 eV therefore indicates that reasonably efficient electron injection from AlSb into ZnTe may be possible, provided that the AlSb layers are heavily doped.

IV. CONCLUSIONS

We have measured the valence band offset in coherently strained Si/Ge (100) heterojunctions as a function of strain, and in AlSb/ZnTe (100) heterojunctions. Our measurements for the Si/Ge system include the first experimental determination of strain-induced shifts in atomic core level to valence band edge binding energies. The values we obtain for the Si/Ge (100) valence band offset are in reasonable agreement with theoretical predictions in which the effects of strain are explicitly incorporated, and are not inconsistent with the postulate that the discontinuity in the weighted average of the strain-split valence bands is independent of strain. Our values are also consistent with experiments in which modulation doping effects were observed in $Si/Si_{1-x}Ge_x$ heterostructures.

For the AlSb/ZnTe (100) heterojunction system, our measurements yield a valence band offset of -0.42 ± 0.07 eV and a conduction band offset of 0.21 ± 0.07 eV. These values are compatible with reasonably efficient electron injection from heavily doped AlSb into ZnTe. Our results also show that a reacted layer containing Al and Te appears to form at the AlSb/ZnTe interface; similar effects have been observed in the GaSb/ZnTe and GaAs/ZnSe heterojunction systems. The effects of this reacted layer on the electronic and structural properties of the interface are unknown but may be important, and are deserving of further study.

ACKNOWLEDGMENTS

We would like to acknowledge useful discussions with R. J. Hauenstein and Y. Rajakarunanayake. One of us (E.T.Y.) is grateful for financial support from the National Science Foundation and the AT&T Foundation. Part of this work was supported by DARPA (monitored by ONR) under Grant No. N00014-86-K-0841 and by ONR under Grant No. N00014-89-J-1141.

[1] J. R. Waldrop, R. W. Grant, S. P. Kowalczyk, and E. A. Kraut, J. Vac. Sci. Technol. A **3**, 835 (1985).
[2] E. T. Yu, D. H. Chow, and T. C. McGill, Phys. Rev. B **38**, 12764 (1988).

[3] J. Tersoff and C. G. Van de Walle, Phys. Rev. Lett. **59**, 946 (1987).
[4] G. P. Schwartz, M. S. Hybertsen, J. Bevk, R. G. Nuzzo, J. P. Mannaerts, and G. J. Gualtieri, Phys. Rev. B **39**, 1235 (1989).
[5] J. H. Van de Merwe, J. Appl. Phys. **34**, 123 (1963).
[6] R. H. Miles, T. C. McGill, P. P. Chow, D. C. Johnson, R. J. Hauenstein, C. W. Nieh, and M. D. Strathman, Appl. Phys. Lett. **52**, 916 (1988).
[7] C. G. Van de Walle and R. M. Martin, Phys. Rev. B **34**, 5621 (1986).
[8] W.-X. Ni, J. Knall, and G. V. Hanson, Phys. Rev. B **36**, 7744 (1987).
[9] Y. Rajakarunanayake and T. C. McGill, Appl. Phys. Lett. **55**, 1537 (1989).
[10] C. L. Yang, D. S. Pan, and R. Somoano, J. Appl. Phys. **65**, 3253 (1989).
[11] J. O. McCaldin and T. C. McGill, J. Vac. Sci. Technol. B **6**, 1360 (1988).
[12] E. T. Croke, T. C. McGill, R. J. Hauenstein, and R. H. Miles, Appl. Phys. Lett. **56**, 367 (1990).
[13] E. A. Kraut, R. W. Grant, J. R. Waldrop, and S. P. Kowalczyk, Phys. Rev. B **28**, 1965 (1983).
[14] M. L. Cohen and T. K. Bergstresser, Phys. Rev. **141**, 789 (1966).
[15] L. R. Saravia and D. Brust, Phys. Rev. **176**, 915 (1968).
[16] J. Chelikowsky, D. J. Chadi, and M. L. Cohen, Phys. Rev. B **8**, 2786 (1973).
[17] L. R. Saravia and D. Brust, Phys. Rev. **178**, 1240 (1969).
[18] *Landolt-Börnstein: Numerical Data and Functional Relationships in Science and Technology* edited by O. Madelung (Springer, New York, 1982), Group III, Vol. 17a.
[19] T. F. Kuech, M. Mäenpää, and S. S. Lau, Appl. Phys. Lett. **39**, 245 (1981).
[20] G. Margaritondo, A. D. Katnani, N. G. Stoffel, R. R. Daniels, and T.-X. Zhao, Solid State Commun. **43**, 163 (1982).
[21] P. H. Mahowald, R. S. List, W. E. Spicer, J. Woicik, and P. Pianetta, J. Vac. Sci. Technol. B **3**, 1252 (1985).
[22] R. People, J. C. Bean, D. V. Lang, A. M. Sergent, H. L. Störmer, K. W. Wecht, R. T. Lynch, and K. Baldwin, Appl. Phys. Lett. **45**, 1231 (1984).
[23] G. Abstreiter, H. Brugger, T. Wolf, H. Jorke, and H. J. Herzog, Phys. Rev. Lett. **54**, 2441 (1985).
[24] G. J. Gualtieri, G. P. Schwartz, R. G. Nuzzo, and W. A. Sunder, Appl. Phys. Lett. **49**, 1037 (1986).
[25] R. W. Grant, E. A. Kraut, S. P. Kowalczyk, and J. R. Waldrop, J. Vac. Sci. Technol. B **1**, 320 (1983).
[26] P. K. Larsen, J. H. Neave, J. F. van der Veen, P. J. Dobson, and B. A. Joyce, Phys. Rev. B **27**, 4966 (1983).
[27] D.-W. Tu and A. Kahn, J. Vac. Sci. Technol. A **3**, 922 (1985).
[28] J. Tersoff, Phys. Rev. Lett. **56**, 2755 (1986).
[29] A. G. Milnes and D. L. Feucht, *Heterojunctions and Metal-Semiconductor Junctions* (Academic, New York, 1972).
[30] W. A. Harrison, J. Vac. Sci. Technol. **14**, 1016 (1977).
[31] W. A. Harrison and J. Tersoff, J. Vac. Sci. Technol. B **4**, 1068 (1986).
[32] S. Subbanna, G. Tuttle, and H. Kroemer, J. Electron. Mater. **17**, 297 (1988).